

10 000 cm^{-1} , where the process analogous to that occurring in the chloride would be expected to be detectable. Further work, preferably involving magnetic circularly polarized emission will be required to identify the excited states involved, but we do not plan to carry out these studies in the near future.

Discussion

The separation of the Γ_7 and Γ_8 components of the ${}^2T_{2g}$ ground state is ${}^3/2\xi$ in the first order. The derived value of ξ in IrCl_6^{2-} and IrBr_6^{2-} is then 3300–3400 cm^{-1} . This is rather larger than expected from other third-row transition elements and supports the view of Allen¹³ that it is essential to include mixing of other crystal field states into the ground state if an accurate spin-orbit coupling parameter is to be obtained.

Of greater interest is the relative intensities of the ν_6 , ν_4 , and ν_3 vibronic origins. Since the ν_6 vibration generates an octapolar field at the metal whereas ν_3 and ν_4 generate dipolar fields, it would be reasonable to suppose that, in the absence of any selection rules, the ν_3 and ν_4 vibronic origins would be much stronger than the ν_6 origin. For d^3 ions Manson¹⁴ has argued that the dipolar term cancels for the ${}^4A_{2g} \rightarrow {}^4T_{2g}$ transition, and this agrees with the experimental observation that the ν_6 vibronic origins have comparable intensity to the ν_4 vibronic origins in $\text{Cr}(\text{NH}_3)_6^{3+}$, MnF_6^{2-} . No similar cancellation occurs for the $\Gamma_7 \rightarrow \Gamma_8$ transition in IrX_6^{2-} and the comparable intensity of the ν_6 and ν_4 vibronic origins remains unexplained.

The main difference between the $\Gamma_8 \rightarrow \Gamma_7$ transitions in the chloride and bromide is that the relative intensities of the ν_1 and ν_2 progressions are reversed. The spectra are insufficiently well resolved for an unambiguous decision as to whether the JTE is in the $\Gamma_8({}^2T_{2g})$ state or a higher odd-parity state. It is of interest however that whereas the $\Gamma_7({}^2T_{2g}) \rightarrow \Gamma_7 + \Gamma_8$ (${}^2T_{2u}$) transition of IrCl_6^{2-} shows evidence of a strong JTE and Ham effect in the excited state, this Ham effect is quenched by the ligand spin-orbit coupling in the IrBr_6^{2-} ion. In this case the active vibration is ν_5 . The different LMCT luminescence behavior of the two ions does point to differences in the ordering of the excited states.

Conclusion

IrCl_6^{2-} and IrBr_6^{2-} show intense luminescence in the infrared ($\Gamma_8({}^2T_{2g}) \rightarrow \Gamma_7({}^2T_{2g})$) and visible (LMCT) regions. The three odd-parity vibrational modes of the octahedron appear strongly in the infrared transition. The potential surfaces of the two states are nearly parallel although there is evidence for a weak Jahn-Teller effect in IrCl_6^{2-} . The detailed assignments of the visible emissions are uncertain.

Acknowledgment. We thank the SRC for financial support.

Registry No. IrCl_6^{2-} , 16918-91-5; IrBr_6^{2-} , 16919-98-5; Cs_2SnCl_6 , 17362-93-5; Rb_2SnCl_6 , 17362-92-4; Cs_2TeCl_6 , 17498-83-8; Cs_2ZrCl_6 , 16918-86-8; Cs_2SnBr_6 , 17362-97-9; Rb_2SnBr_6 , 17362-96-8; Cs_2TeBr_6 , 16925-33-0; Cs_2ZrBr_6 , 36407-58-6.

Contribution from the Department of Chemistry, University of Sydney, New South Wales 2006, Australia, and the University Leicester, Leicester, England

Single-Crystal Raman Spectroscopic Study of Apophyllite, a Layer Silicate

DAVID M. ADAMS,*^{1a} ROBERT S. ARMSTRONG,^{1b} and STEPHEN P. BEST^{1b}

Received September 19, 1980

Good-quality single-crystal Raman data have been obtained at both ambient temperature and 100 K for an oriented crystal of apophyllite, $\text{KCa}_4(\text{Si}_4\text{O}_{10})_2(\text{F}/\text{OH})\cdot 8\text{H}_2\text{O}$, a layer structure silicate with four- and eight-membered rings. The numbers of bands found for each symmetry species closely approximate those predicted by factor group analysis. An A_{1g} mode at 109 cm^{-1} is attributed principally to Ca^{2+} translatory motion, with the implication that bands at similar positions in B_{1g} , B_{2g} , and E_g spectra are of similar provenance. Some regions of the spectrum show pronounced thermal dependence and are tentatively associated with movements of lattice water. The $\nu(\text{OH})$ region bands are attributed entirely to the lattice water, the sharp bands near 3560 cm^{-1} arising from short, non-hydrogen-bonded O-H motion and the broad ones from hydrogen-bonded lattice water O-H bonds.

Introduction

The marvelous variety of structures, based upon the SiO_4 tetrahedral unit, presented by silicates poses many challenging problems in vibrational spectroscopy. Much effort has been expended upon the IR spectroscopy of these materials but rather little upon Raman investigations; and excellent summary of the field is given in Farmer's book.² For a further understanding of the usually highly complex vibrational spectra of silicates beyond the level possible from IR spectroscopy of powders, aided and abetted by normal-coordinate analysis, data must be collected from oriented single crystals with use of linearly polarized radiation. By these means, securely based assignments have recently been obtained for several orthosilicates,³⁻⁶ and believable accounts of some pyrosilicates are

on record.² Studies of chain⁶⁻⁸ and ring silicates⁹⁻¹¹ are also becoming increasingly common. There remains, however, a particular need for detailed analyses of the more complex sheet and framework structural types. For this reason we have undertaken a single-crystal Raman study of apophyllite. This mineral has an unusual layer structure in which SiO_4 tetrahedra form four- and eight-membered rings. Comparable sheets are found in gillespite, $\text{BaFeSi}_4\text{O}_{10}$, and in Egyptian blue, $\text{CaCuSi}_4\text{O}_{10}$. All three materials present intriguing structural and phase-stability problems. Apophyllite is also quite heavily hydrated. The precise forms of protonated moiety present continue to be a matter of debate. The problem is

- (1) (a) University of Leicester. (b) University of Sydney.
- (2) V. C. Farmer, Ed., "The Infrared Spectra of Minerals", Mineralogical Society, London, 1974.
- (3) V. Hohler and E. Funck, *Z. Naturforsch., B: Anorg. Chem., Org. Chem.*, **29B**, 340 (1974).
- (4) V. Devarajan and E. Funck, *J. Chem. Phys.*, **62**, 3406 (1975).
- (5) H. D. Stidham, J. B. Bates, and C. B. Finch, *J. Phys. Chem.*, **80**, 1226 (1976).

- (6) D. M. Adams and D. J. Hills, *J. Chem. Soc., Dalton Trans.*, 1562 (1977).
- (7) V. Devarajan and H. F. Shurvell, *Can. J. Chem.*, **55**, 2559 (1977).
- (8) N. O. Zulumyan, A. P. Mirgorodskii, V. F. Pavinich, and A. N. Lazarev, *Opt. Spektrosk.*, **41**, 1056 (1976).
- (9) D. M. Adams and I. R. Gardner, *J. Chem. Soc., Dalton Trans.*, 1502 (1974).
- (10) D. M. Adams and I. R. Gardner, *J. Chem. Soc., Dalton Trans.*, 315 (1976).
- (11) F. Gervais and B. Piriou, *C. R. Hebd. Seances Acad. Sci., Ser. B*, **274**, 252 (1972).

Table I. Factor Group Analysis^a for Apophyllite, $[\text{KCa}_4(\text{Si}_4\text{O}_{10})_2(\text{F}/\text{OH})\cdot 8\text{H}_2\text{O}]_2$

		D_{4h}									
		A_{1g}	A_{2g}	B_{1g}	B_{2g}	E_g	A_{1u}	A_{2u}	B_{1u}	B_{2u}	E_g
K	2b						1	1	0	0	2
Ca	8h	2	2	2	2	2	1	1	1	1	4
Si	16i	3	3	3	3	6	3	3	3	3	6
O _I	8g	1	2	2	1	3	1	2	2	1	3
O _{II,III}	2 × 16i	6	6	6	6	12	6	6	6	6	12
F	2a						1	1	0	0	2
$N(\text{total})$		12	13	13	12	23	13	14	12	11	29
T_A							0	1	0	0	1
T		2	3	2	2	3	3	3	1	1	8
$\Gamma(\text{sheets})$		10	10	11	10	20	10	10	11	10	20
$\nu(\text{Si-O}_{III})_t$		1	1	1	1	2	1	1	1	1	2
$\nu(\text{Si-O}_{II})_b$		1	1	1	1	2	1	1	1	1	2
$\nu(\text{Si-O}_I)_b$		1	0	0	1	1	1	0	0	1	1
activities		$x^2 + y^2, z^2$		$x^2 - y^2$	xy	(xz, yz)		z			(x, y)

(B) Additional Modes Contributed by Water Molecules

		$N(\text{total})$									
		9	9	9	9	18	9	9	9	9	18
$\nu(\text{OH})$		2	2	2	2	4	2	2	2	2	4
$\delta(\text{HOH})$		1	1	1	1	2	1	1	1	1	2
$T(\text{H}_2\text{O})$		3	3	3	3	6	3	3	3	3	6
$R(\text{H}_2\text{O})$		3	3	3	3	6	3	3	3	3	6

^a T_A = acoustic and T = optic branch translatory modes. $\Gamma(\text{sheet})$ = internal modes of silicate framework. $T(\text{H}_2\text{O})$ and $R(\text{H}_2\text{O})$ are external modes of water of translatory and libratory (equivalent representations from ρ_ω , ρ_T , and ρ_r) types, respectively.

outlined below in the course of the Discussion. There have been no previous single-crystal Raman studies of apophyllite, but Vierne and Brunel have reported mid-IR reflectance spectra.¹²

Theory

The structure of apophyllite was correctly solved in 1931.¹³ Subsequent reinvestigations by X-ray^{14,15} and neutron^{16,17} diffraction, while confirming the original structure, have also located proton positions, although their interpretation is not entirely settled.

This mineral adopts the tetragonal space group symmetry $P4/mnc = D_{4h}^2$, $Z = 2$. The ideal formula is $\text{KCa}_4(\text{Si}_4\text{O}_{10})_2(\text{F}/\text{OH})\cdot 8\text{H}_2\text{O}$. There are two sheets per unit cell, normal to the c axis. Water molecules lie in the sheets. Of the interlayer cations, potassium is surrounded by eight water molecules and calcium by both water and silicate oxygen atoms. On this basis we regard the bonding between the cations and the rest of the structure as primarily ionic in type and therefore are justified in decomposing the vibrational representation spanned by $N(\text{total})$ (Table I) into contributions from the mode types shown.

The factor group analysis (fga) (Table I) reveals a number of important facts.

First, it is seen that the translatory motions of K^+ and F^- do not contribute to the Raman spectrum. Thus, the only translatory modes which may contribute to the Raman spectrum are due to Ca^{2+} and to the three modes (A_{2g} and E_g) in which the silicate sheets move relative to each other. Since the T_{1u} phonon frequency in CaO is 290 cm^{-1} ¹⁸ and Ca^{2+} in

Table II. Correlation of Layer Modes for Apophyllite

isolated ring C_4	$\times 2$ \rightarrow	isolated layer D_4	$\times 2$ \rightarrow	unit cell ^a D_{4h}^2
A (Raman, IR) {		A_1 (Raman)		$A_{1g} + A_{1u}$
		A_2 (IR)		$A_{2g} + A_{2u}$
B (Raman) {		B_1 (Raman)		$B_{1g} + B_{1u}$
		B_2 (Raman)		$B_{2g} + B_{2u}$
E (Raman, IR)		E (Raman, IR)		$E_g + E_u$

^a Activities are given in Table IA.

apophyllite is bonded to a mixture of water and silicate oxygen atoms, it is unlikely that these translatory modes will be $>250\text{ cm}^{-1}$. The translatory mode in which the two silicate sheets move apart parallel to the c axis is of A_{2g} symmetry and is therefore inactive. The Raman-active E_g mode, in which motion is constrained to the x,y plane, is a "rigid layer shear" mode (rls). Such modes are always of very low frequency. In apophyllite the two silicate layers are separated by a layer of largely aquated cations and it is expected that the rls mode will be the lowest E_g mode observed.

The silicon and oxygen motions contribute to all symmetry species. Nevertheless, the group-theoretical arguments allow much about the spectrum of the framework to be deduced. Each silicate sheet has the symmetry elements: $\{E|0\}$, $2\{C_4(z)|0\}$, $\{C_2(z)|0\}$, $2\{C_2^{1/2}(a+b)\}$, and $2\{C_2^{1/2}(a/2)\}$. They define a group isomorphous with D_4 . Since the sheets are physically separated from each other, it is to be expected that the unit cell spectrum will be well represented by that of a single D_4 sheet with a fairly small correlation perturbation. Moreover, each D_4 sheet consists of two fourfold rings of C_4 symmetry and it is reasonable to suppose that the coupling of these rings will be reflected in the construction of the spectrum. Details of these two levels of coupling are in Table II. From this it follows that correlation coupling between sheets will be apparent only by virtue of any frequency differences observed

(12) R. Vierne and R. Brunel, *Bull. Soc. Fr. Mineral. Crystallogr.*, **92**, 409 (1969).

(13) W. H. Taylor and St. Naray-Szabo, *Z. Kristallogr., Kristallgeom., Kristallphys., Kristallchem.*, **77**, 146 (1931).

(14) A. A. Colville, C. P. Anderson, and P. M. Black, *Am. Mineral.*, **56**, 1222 (1971).

(15) G. Y. Chao, *Am. Mineral.*, **56**, 1234 (1971).

(16) E. Prince, *Am. Mineral.*, **56**, 1243 (1971).

(17) H. Bartl and G. Pfeifer, *Neues Jahrb. Mineral. Monatsh.*, **58** (1976).

(18) S. D. Ross, "Inorganic Infrared and Raman Spectra", McGraw-Hill, London, 1972.

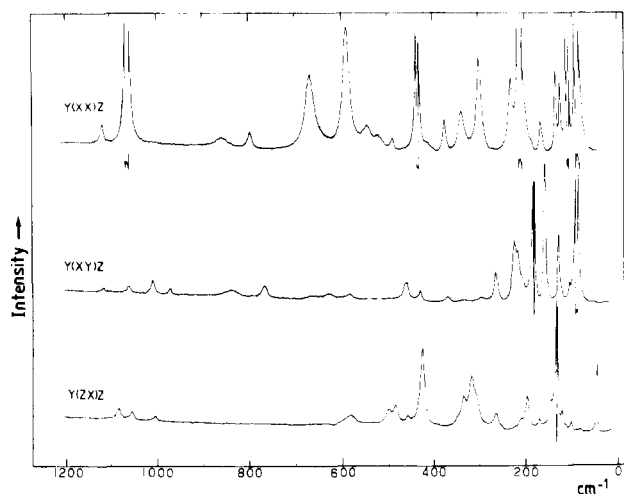


Figure 1. Single-crystal Raman spectra of apophyllite at ambient temperature (spectral bandwidth 2.3 cm^{-1} at 600 cm^{-1} ; sensitivity $10^3 \text{ counts s}^{-1}$ ($10^4 \text{ counts s}^{-1}$ in off-scale regions); 300-mW, 514.5-nm radiation at the sample).

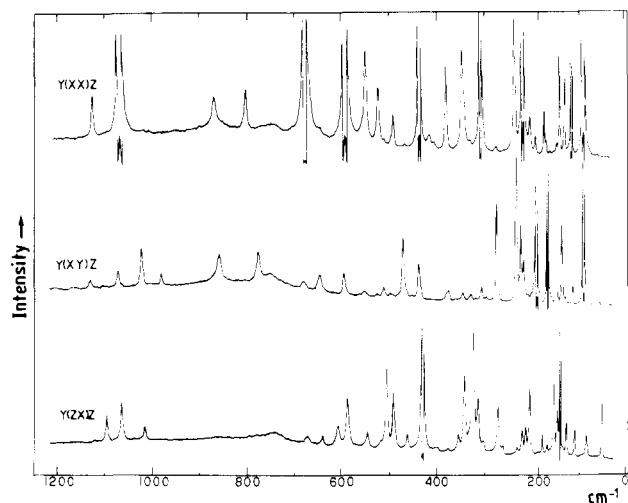


Figure 2. Single-crystal Raman spectra of apophyllite at 100 K (conditions as for Figure 1).

between the E_g Raman and the E_u IR spectra: this follows because all other Raman-active species correlate to inactive u-type modes. Thus, insofar as our Raman spectra are concerned, they may be treated as reflecting the vibrational modes of a single silicate layer.

In addition to the framework vibrations, water molecules will generate bands due to translatory and libratory modes; established assignments for ice and highly hydrated materials suggest that these will be found in the ranges 200–300 and 400–900 cm^{-1} , respectively. Finally, if hydroxyl groups are present, they will contribute libratory and translatory modes: these are expected in the regions 800–1200 and $<600 \text{ cm}^{-1}$, respectively.

Experimental Section

A well-formed, colorless single crystal of apophyllite in the shape of a faceted cube of side ca. 3 mm was obtained from the Australian National Museum, Sydney, through the courtesy of Mr. Lindsay Sutherland. Unusually, the crystal was free of the milky white appearance typical of apophyllite, thus rendering it suitable for Raman study. It was also largely free from laser-induced fluorescence which so often precludes Raman work with minerals.

The crystal showed perfect (001) cleavage and well-developed (110) faces. Excellent spectra were obtained in experiments $y'(ij)z$, and supplemented by others of the type $x'(ij)y'$ in order to permit separation of A_{1g} and B_{2g} modes (Table III). Low-temperature spectra were

Table III. Scattering Geometries Used and Tensor Components Excited

$y'(ij)z$		$x'(ij)y'$	
$y'(x'x')z$	$A_{1g} + B_{2g}$	$x'(zz)y'$	A_{1g}
$y'(x'y')z$	B_{1g}	$x'(y'x')y'$	B_{1g}
$y'(zx')z$	} E_g	$x'(y'z)y'$	} E_g
$y'(zy')z$		$x'(zx')y'$	

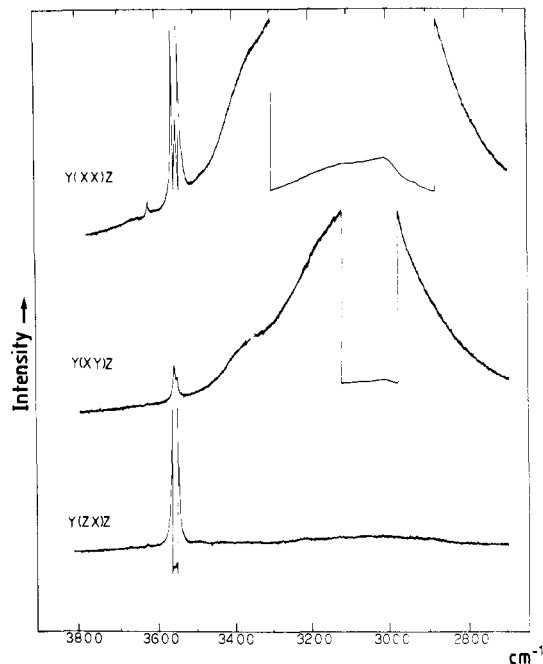


Figure 3. Single-crystal Raman Spectra of apophyllite in the $\nu(\text{OH})$ region at ambient temperature (spectral bandwidth 2.6 cm^{-1} at 3000 cm^{-1} ; sensitivity $10^3 \text{ counts s}^{-1}$; 460-mW, 514.5-nm radiation at the sample).

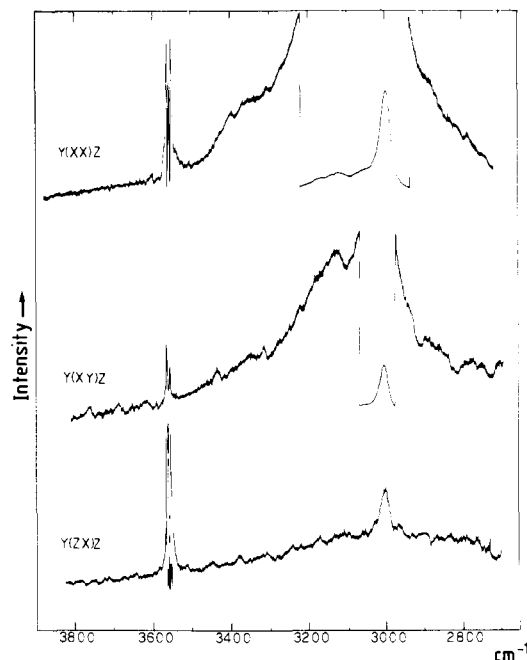


Figure 4. Single-crystal Raman spectra of apophyllite in the $\nu(\text{OH})$ region at 100 K (conditions as for Figure 3).

obtained with the sample mounted in an Oxford Instruments CF100 cryostat.

Spectra were excited with 514.5-nm radiation from an argon ion laser and recorded with use of a Spex 1401 double monochromator

Table IV. Raman Wavenumbers and Photon Count Rates (Units of 10^2 s^{-1}) for Apophyllite at Liquid Nitrogen (A) and Ambient (B) Temperatures

ν/cm^{-1}	A			B			ν/cm^{-1}
	$y'(x'x')z$ $A_{1g} + B_{2g}$	$y'(x'y')z$ B_{1g}	$y'(zx')z$ E_g	$y'(zx')z$ E_g	$y'(x'y')z$ B_{1g}	$y'(x'x')z$ $A_{1g} + B_{2g}$	
1122	12				2	10	} 1117
1120		2					
1096			5	6			1090
1062 ^a	132					120	1061 ^a
1013		9.5			7.5		1009
1012			2.3	2			1010
997			2				
971		2.5			3		972
860	12					4	856
849		7			2.5		~841
796	15					6.5	793
766		6.5			5		767
673	54					12.5	664
639			1.5				
637		2.2			2		628
605			2.7				
589 ^a	128					65	584 ^a
545 ^a	29		3			12	542 ^a
520	17					7	~517
506			12	8			504
491			7	10			489
487 ^a	10					6	487 ^a
464		10			9		464
462			2.5	2.5			462
431	136	10				107	432
430			47	42			
419 ^a	3						
410 ^a	3						
399 ^a	2						
379	25					18.5	374
375		2			2.8		373
355	3		2.5	4			~355
343	30						
342			13	18			340
341		2			1	22	338
325			21	29			322
312			12	8			312
304	75					50	299
273			8	7			270
270		29			16		267
259		2					
234	46					43	231
229		56.5			36		226
220			4				
219		27			26		219
213	190	13				147	210
206			12	20			203
199	22						
187		122			10	2	186
178			3	4			177
169 ^a	17		3			16	166 ^a
163		100			88		162
155			13	15			152
147			10				
141			43	89			139
137	46					47	134
134		36			37		130
128			7.5	9			127
126	35					35	124
109 ^a	110					150	107 ^a
81	240					170	87
88		125			109		92
75		1.5					
51			15	41			52

^a A_{1g} modes, determined from $x'(ij)y'$ experiments.

with an RCA 31034A GaAs photomultiplier tube and photon counting.

Results and Discussion

Data are shown in Table IV and Figures 1–4. From the figures it is seen that extinctions between the spectra generated

by the various tensor components are generally good, particularly for the room-temperature spectra. Some slight leakage is evident for the strongest bands, but this does not give rise to any ambiguity except in the case of the band at 432 cm^{-1} . Here the intensity in both B_{2g} and E_g spectra, coupled with

the good extinctions elsewhere, plainly shows that two modes of differing symmetry species are coincident. It is not, however, clear whether the low intensity also present at this energy in the B_{1g} spectrum is due to a genuine B_{1g} mode or to leakage from the others. In the $\nu(\text{Si-O})$ region the intense 1061-cm^{-1} A_{1g} band breaks through into the other spectra but this is easily recognized.

$\nu(\text{Si-O})$ Region. The most significant deficiency of the results is that only one of the three expected A_{1g} modes appears in the range $600\text{--}1200\text{ cm}^{-1}$: this must be attributed to accidental weakness. However, the polarized IR reflectance data of Vierre and Brunel,¹² confirmed by our own recent observations, show that there are two A_{2u} modes, at 1048 and 1129 cm^{-1} . The significance of this observation is that it shows that both the Si-O bridge and terminal bonds yield stretching frequencies at comparable energies.

The Raman spectrum shows only three of the predicted five E_g modes in the $600\text{--}1200\text{-cm}^{-1}$ region at ambient temperature, although two weak bands appear at 605 and 639 cm^{-1} on cooling. These we consider to be far too low to be $\nu(\text{Si-O})$ modes. The polarized IR reflectance spectrum similarly shows only three E_u bands (1015 , 1095 , and 1120 cm^{-1}), until a weak doublet at 785 , 762 cm^{-1} , of which both members are E_u in type. The scheme of coupling between the two sheets, Table II, shows that the E_g and E_u modes should occur near each other. This is clearly the case at $>970\text{ cm}^{-1}$, but it is significant that there are no E_g bands analogous to the E_u pair, which are near 790 cm^{-1} in the IR spectrum. Thus, either the bands near 790 cm^{-1} (in both Raman and IR spectra) are not $\nu(\text{Si-O})$ or there are vanishingly weak E_g modes in this region. If coupling of the two C_4 fourfold rings per layer is weak, and/or the coupling between the two layers (Table II) is weak, accidental coincidence of two E_g modes is to be expected (the same applies for E_u modes), thus accounting for observation of less than the full theoretical number of bands $>970\text{ cm}^{-1}$. The correctness of this explanation cannot be proved without further IR work in polarized light. We note, however, that placing all $\nu(\text{Si-O})$ modes $>900\text{ cm}^{-1}$ is in accord with recent assignments for ring silicates, which also have both terminal and bridged Si-O bonds.⁹⁻¹¹ However, in apophyllite it is not impossible that Si-O-Ca bonds will give rise to $\nu(\text{Si-O})$ modes at somewhat lower frequencies. There are broad features in the $y'(x'x')z$ and $y'(x'y')z$ spectra at ca. 841 and 856 cm^{-1} at room temperature which sharpen on cooling to 100 K to give peaks at 849 and 860 cm^{-1} , respectively. It is unusual for silicate spectra to show such pronounced thermal dependence. We tentatively conclude that the features ca. 850 cm^{-1} are associated with either OH^- or water librations; we hope to test this hypothesis eventually by deuteration of a sample of apophyllite.

The Region below 800 cm^{-1} . On the assumption that the assignments for the region $>800\text{ cm}^{-1}$ are correct, Table I shows that the following numbers of bands should be found below 800 cm^{-1} , neglecting for the moment modes due to libration and translation of water molecules:

	$A_{1g} +$ B_{2g}	A_{1g}	B_{1g}	B_{2g}	E_g
theory	20	9	9	11	18
expt (100 K)	22	8	14	14	21

The most obvious conclusion is that, for all but A_{1g} species, more bands are found than are required by theory. However, the band count includes several very weak features whose status is ambiguous. They may arise from impurity-induced modes, a probable feature of mineral spectra. Alternatively, they may be due to second-order features or, in a few cases, have been incorrectly identified as fundamentals whereas they may be due to leakage from another symmetry species. Third,

any bands that show marked thermal sensitivity must be regarded as good candidates for assignment to external modes of water if they occur in the energy regions indicated in the Theory.

Despite these qualifications, which are examined more fully below, the major conclusion is not in doubt: that the observed spectra correspond closely to the predictions of fga, despite the substantial size of the unit cell.

In the A_{1g} spectrum there are bands at 109 and 169 cm^{-1} but no others until at least 400 cm^{-1} . It is therefore reasonable to assign the lower of these bands to one of the two Ca^{2+} translatory modes expected in the A_{1g} spectrum. If this is correct, then the fga requires that bands should also be found at similar frequencies in each of the other spectra. A unique choice cannot be made, however, as for each of the other symmetry species there are several bands in this region. It is evident that the silicate sheet has many low-lying deformational motions so that these must interact substantially with the Ca^{2+} translational motions so that, in fact, all modes below ca. 200 cm^{-1} will be of mixed character for these species. Nevertheless, these new data provide, for the first time, an unequivocal sort into symmetry species of the many vibrational frequencies of this complex material, upon which a normal-coordinate analysis may now be attempted, although it would be wise to defer this until full single-crystal IR data have been obtained.

Several low-frequency regions of the Raman spectra of apophyllite show pronounced thermal dependence. They are $200\text{--}250$, $300\text{--}360$ (in E_g), and $400\text{--}550\text{ cm}^{-1}$. Until deuterated apophyllite has been made, it is premature to attempt detailed assessment of this evidence. Nevertheless, we consider it probable that all these regions are associated either with external motions of water or with parts of the sheet framework which are affected by the ordering of the water. If all the thermally sensitive bands are attributed to external modes of water, there is a deficiency of bands arising from the framework. We consider it more probable that the majority of the observed bands are from the framework. The lowest observed mode is of E_g type (51 cm^{-1}) and is probably the rls mode.

The $\nu(\text{OH})$ and $\delta(\text{HOH})$ Regions. The $\nu(\text{OH})$ bands observed at ambient temperature sit up on a broad fluorescence background which is greatly reduced on cooling to 100 K , (Figure 3 and 4). At neither temperature were bands found in the $\delta(\text{HOH})$ region, apart from a few broad features at 100 K , which are most probably fluorescence fine structure.

Two neutron diffraction studies^{16,17} have established that the water molecules in apophyllite are hydrogen bonded to the silicate framework. There remains, however, serious disagreement. Prince¹⁶ suggests that the structural formula is $\text{KCa}_4(\text{Si}_4\text{O}_{10})_2\text{F}_{1-x}(\text{HF})_x(\text{H}_2\text{O})_{8-x}(\text{OH})_x$. In his model approximately one-eighth of the water molecules are replaced by OH^- and the remaining protons bonded to fluoride to form HF molecules. Both OH^- and H_2O are hydrogen bonded to the silicate framework. More recently, Bartl and Pfeifer¹⁷ have claimed that the true situation is more properly represented by the formula $\text{KCa}_4(\text{Si}_4\text{O}_{10})_2(\text{F}/\text{OH})\cdot 8\text{H}_2\text{O}$, where hydroxyl has been partly substituted for fluoride. Thus, in this model, the extra electron density near fluoride is identified as due to the proton of OH^- rather than of HF. This is highly likely in view of the known ability of fluoride and hydroxyl to replace each other in minerals such as apatite. It also avoids the need to account for the very long H-F distance (1.03 \AA) which Prince found for "HF" in the crystal, as compared with the gas-phase value, 0.91 \AA . In the gas phase $\nu(\text{HF})$ is at 4138 cm^{-1} .¹⁹ No Raman band was found for apophyllite either near this value or at lower values, until the $\nu(\text{OH})$ region, thus

(19) K. Nakamoto, "Infrared and Raman Spectra of Inorganic and Coordination Compounds", 3rd ed., Wiley-Interscience, New York, 1978.

supporting the more recent structure. The Raman spectra in this region are closely paralleled by the IR spectra,²⁰ which also show a sharp doublet (3570, 3580 cm⁻¹) followed at lower frequencies by two very broad, complex regions of absorption. The broad bands are undoubtedly due to strongly hydrogen-bonded water, but the sharp bands might arise either from hydroxyl (which substitutes for fluoride in the lattice) or from the shorter of the two O-H bonds in the water molecules (0.953 and 0.983 Å, respectively¹⁷).

Hydroxyl groups in apophyllite occupy Wyckoff sites 4e (0, 0, z; etc.), lying along the fourfold axis but disordered with respect to ±z. This would generate the representation

$$A_{1g}(\text{Raman}) + A_{2g}(\text{inact.}) + A_{1u}(\text{inact.}) + A_{2u}(\text{IR})$$

which plainly does not account for the spectra, most notably for the presence of a doublet in the E_g spectrum. We conclude that the sharp ν(OH) features arise from motion of the shorter of the two bonds of the lattice water. ν(OH) of hydroxyl was

not detected, we suggest, because of its low concentration: most apophyllites are fluorine rich.²¹

A set of 16 symmetry-related short O-H bonds on general positions generates half the representation shown as the row "ν(OH)" in Table IB. Thus, appearance of a doublet (3550, 3557 cm⁻¹) in the E_g spectrum is accounted for, as is presence of intensity in both B_{1g} and A_{1g}/B_{2g} (3558 cm⁻¹) spectra (Figure 3 and 4). The same selection rules apply for the set of 16 long O-H bonds: the results show ν(OH) intensity below 3400 cm⁻¹ for all symmetry species, in accord with these rules. A detailed assignment is not attempted for these bands as δ(OH₂) overtones almost certainly complicate the situation.

Acknowledgment. We thank the Foundation for Inorganic Chemistry within the University of Sydney for sponsoring appointment of D.M.A. as Visiting Professor in 1979, during which this work was done.

Registry No. Apophyllite, 58572-15-9.

(20) H. Moenke, "Mineralspektren," Akademie-Verlag, Berlin, 1962.

(21) G. F. Marriner, J. I. Langford, and J. Tarney, *J. Appl. Cryst.*, **12**, 131 (1979).

Contribution from the Department of Applied Science, Faculty of Engineering, Tohoku University, Sendai, Japan

Vibrational Spectra of Trimethylphosphine Telluride and the P-Te Stretching Force Constant

FUMIO WATARI*

Received August 25, 1980

The infrared (4000-400 cm⁻¹) and Raman (3200-100 cm⁻¹) spectra of (CH₃)₃PTe and (CD₃)₃PTe have been recorded for the solid state. The solution Raman spectra also have been recorded. The spectra have been interpreted on the basis of C_{3v} molecular symmetry. Normal-coordinate analysis has been carried out in terms of symmetry force constants. The PC₃ degenerate stretch was found to be mixed with the CD₃ rocks in (CD₃)₃PTe; therefore its assignment was not unequivocal. The P-Te force constant was found to have a value of 2.20 mdyne/Å which is compared with the P-O, P-S, and P-Se force constants in the trimethylphosphine chalcogenides.

Introduction

Although numerous alkyl- and arylphosphine compounds with oxygen, sulfur, and selenium are well-known, phosphine telluride, which is the next homologue to the selenide, is little known. The first example of trialkylphosphine telluride is tributylphosphine telluride prepared by Zingaro.¹ Subsequently several phosphine tellurides have been prepared by the reaction of tellurium with phosphines.² Chremos and Zingaro³ have examined the location of the P-Te stretching vibration for some phosphine tellurides (C_nH_{2n+1})₃PTe (n = 3-5 and 8) and observed a doublet, one peak around 400 and the other around 450 cm⁻¹. These frequencies are confined in a rather narrow range, even though the P-Se frequency in trialkylphosphine selenides shows dependence on alkyl substituents.⁴ The P-Te stretching vibration in tris(dimethylamino)phosphine telluride has been assigned to 519 cm⁻¹, and the force constant has been determined to be 5.89 mdyne/Å, in spite of the P-S force constant being 3.81 mdyne/Å in the corresponding sulfide.⁵ Thus, it was felt that precise vibrational analysis would be necessary to place the P-Te vibration and to determine its force constant. However the above compounds containing many atoms are structurally complex and make the analysis intractable.

In a previous paper,⁶ the vibrational analyses of (CH₃)₃PO, (CH₃)₃PS, and (CH₃)₃PSe have been reported. This work is also an extension of the vibrational study to the telluride. Trimethylphosphine telluride is the simplest molecule of the phosphine tellurides and convenient for elucidating the P-Te stretching frequency and force constant. Preparation of trimethylphosphine telluride is simple,⁷ but it is unstable, which makes the recording of the vibrational spectra difficult by conventional procedures. This difficulty was overcome with the aid of a special sampling technique.

Experimental Section

Infrared Samples. Tellurium was sublimed onto a CsI optical plate in vacuo in an appropriate glass tube. The plate coated with thin film of tellurium was fixed in a low-temperature cell with a small side tube of trimethylphosphine, and after evacuating it and subsequent cooling of the plate with liquid nitrogen, trimethylphosphine was condensed on the tellurium film. The CsI plate was then warmed by expelling

* Address correspondence to the Department of Resource Chemistry, Faculty of Engineering, Iwate University, Morioka, Iwate.

- (1) Zingaro, R. A. *J. Organomet. Chem.* **1963**, *1*, 200.
- (2) Zingaro, R. A.; Steeves, B. H.; Irgolic, K. *J. Organomet. Chem.* **1965**, *4*, 320.
- (3) Chremos, G. N.; Zingaro, R. A. *J. Organomet. Chem.* **1970**, *22*, 637.
- (4) Zingaro, R. A. *Inorg. Chem.* **1963**, *2*, 192.
- (5) Raeuchle, F.; Pohl, W.; Blaich, B.; Goubeau, J. *Ber. Bunsenges. Phys. Chem.* **1971**, *75*, 66.
- (6) Watari, F.; Takayama, E.; Aida, K. *J. Mol. Struct.* **1979**, *55*, 169.
- (7) Brodie, A. M.; Rodley, G. A.; Wilkins, C. J. *J. Chem. Soc. A* **1969**, 2927.